Hindawi
International Journal of Antennas and Propagation
Volume 2019, Article ID 7380621, 8 pages
https://doi.org/10.1155/2019/7380621

Research Article

Compact Wideband Dual-Frequency Antenna Based on a Simplified Composite Right/Left-Handed Transmission Line with Hilbert Curve Loading

Tianpeng Li, Jian Zhang, Baowei Cheng, Xue Lei, Zhijian Xu, and Jun Gao

PLA Strategic Support Army Information Engineering University, Zhengzhou, Henan 450000, China

Correspondence should be addressed to Baowei Cheng; 270822214@qq.com

Received 6 July 2019; Revised 20 October 2019; Accepted 30 October 2019; Published 27 December 2019

Academic Editor: Laura Corchia

This paper addresses the issues of low bandwidth, gain, and efficiency of miniaturized microwave antennas by proposing a novel wideband dual-frequency coplanar waveguide antenna design based on a simplified composite right/left-handed (SCRLH) transmission line structure with Hilbert curve loading. The multifrequency characteristics of the SCRLH transmission line structure are evaluated theoretically, and the antenna parameters promoting bandwidth broadening under zeroth-order resonance (ZOR) and first-order resonance (FOR) mode operation are evaluated. The bandwidth broadening in the ZOR and FOR modes is accordingly revealed to be independent of the antenna length, and the structure therefore facilitates wideband operation under miniaturization. Finally, the dual-frequency ZOR and FOR mode antenna design with center frequencies of $f_0 = 1.865$ GHz and $f_1 = 2.835$ GHz is validated via simulation, and the performance of a compact prototype antenna is evaluated experimentally. The −10 dB return loss bandwidths at f_0 and f_1 are 187 MHz (from 1.773 GHz to 1.96 GHz) and 368 MHz (from 3.002 GHz to 3.37 GHz), and the corresponding relative bandwidths are 10.1% and 11.5%, respectively. The experimentally measured peak gains and radiation efficiencies at f_0 are 1.54 dB and 81.3%, respectively, and those at f_1 are 1.71 dB and 74.2%, respectively.

1. Introduction

Wireless communication systems have been increasingly subjected to the parallel development trends of miniaturization and integration in both military and civilian applications [1]. However, this is particularly problematic when integrating antennas with miniaturized wireless communication devices because they invariably degrade the performance of the antenna, such as by narrowing the bandwidth and deteriorating the directivity pattern. In addition, an increasing state of technological development creates increasingly scarce spectrum resources while increasing the demand for higher communication quality. These conditions collectively require communication systems to work efficiently in different frequency bands. Therefore, the development of compact wideband dual-frequency antenna designs that support or even improve antenna performance is essential to meet the increasingly stringent requirements of wireless communication systems [2–4].

Excellent multifrequency antenna performance has been achieved by antennas based on composite right/left-handed (CRLH) transmission lines owing to their unique dispersion controllability and the capability of controlling their negative-, zeroth-, and positive-order resonance frequencies. For example, Narieda et al. [5] proposed a coplanar waveguide (CPW) dual-frequency antenna design based on a one-dimensional CRLH transmission line structure using the zeroth-order resonance (ZOR) mode and the positive first-order resonance (FOR) mode. Gummalla et al. [6] proposed a three-frequency antenna based on a two-dimensional CRLH transmission line using the ZOR, positive FOR, and positive second-order resonance modes. However, while these past studies have both achieved multifrequency antenna performance, the antenna designs suffered from unacceptably narrow bandwidths.

As a means of addressing the issue of bandwidth narrowing, continuing CRLH transmission line research has increasingly focused on new forms, such as negative dielectric constant (i.e., ε-negative (ENG)) transmission lines and negative magnetic permeability (i.e., μ-negative (MNG)) transmission lines. Because both ENG and MNG transmission lines can be regarded as the result of removing the series capacitance or the shunt inductance of a CRLH transmission line, some researchers have denoted these designs as simplified CRLH (SCRLH) transmission lines [7, 8]. However, current efforts in this area suffer from deficiencies, such as low peak gain, degraded directivity, and low radiation efficiency.

This paper addresses these issues by proposing a new wideband dual-frequency CPW antenna design based on an SCRLH transmission line structure with Hilbert curve loading. The multifrequency characteristics of the SCRLH transmission line structure are evaluated theoretically, and the antenna parameters promoting bandwidth broadening under ZOR and FOR mode operation are evaluated. The analysis reveals that the bandwidth broadening of the ZOR and FOR modes is independent of the antenna length, and the SCRLH transmission line structure therefore facilitates wideband operation under miniaturization. Finally, the dual-frequency ZOR and FOR mode antenna design is validated via simulation, and the performance of a compact prototype antenna is evaluated experimentally. The experimental results are found to be in excellent agreement with the simulation results and thereby validate the proposed antenna design.

2. Bandwidth Broadening Based on an SCRLH Transmission Line

Figure 1 shows an equivalent circuit of a single SCRLH transmission line unit structure of length d consisting of a series-connected right-handed inductor L_R, a shunt left-handed inductor L_L, and a shunt right-handed capacitor C_R.

As discussed, the equivalent circuit in Figure 1 differs from that of a standard CRLH transmission line only in that it has omitted a series left-handed capacitor. Applying the Bloch–Floquet theorem to a single SCRLH transmission line unit yields the following dispersion equation [9]:

$$\beta(\omega) = \frac{1}{d}\cos^{-1}\left(1 - \frac{\omega^2}{2\omega_R^2} + \frac{\omega_E^2}{2\omega_R^2}\right), \tag{1}$$

where $\omega_E = 1/\sqrt{L_L C_R}$ is the resonance frequency of the shunt branch of the equivalent circuit and $\omega_R = 1/\sqrt{L_R C_R}$ is the resonance frequency of the right-handed part of the equivalent circuit. For a multiunit SCRLH transmission line of length l and a signal wavelength λ, the resonance order n, phase constant β_n, number of units N, and unit length d satisfy the following relationship:

$$\theta = \beta_n l = \beta_n N d = \frac{2\pi}{\lambda}\frac{n\lambda}{2} = n\pi. \tag{2}$$

Solving equations (1) and (2) simultaneously yields the following expression for the resonance frequencies of an SCRLH transmission line:

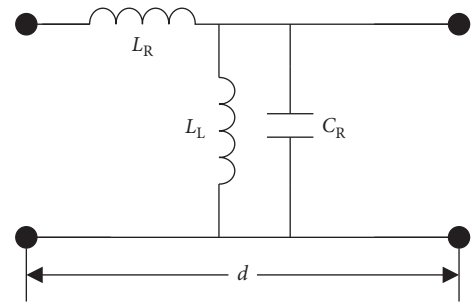

Figure 1: Equivalent circuit of a single SCRLH transmission line unit of length d.

$$\omega_n = \sqrt{\frac{1}{C_R}\left(\frac{1}{L_L} + \frac{2}{L_R} - \frac{2}{L_R}\cos\frac{n\pi}{N}\right)}. \tag{3}$$

In equations (2) and (3), $n = 0, 1, 2, \ldots, N-1$, indicating that the SCRLH transmission line has one ZOR mode and $N-1$ positive resonance modes, for a total of N resonance modes. This differs from conventional right-handed transmission lines and pure left-handed transmission lines and is the very reason that a CRLH transmission line is capable of multifrequency operation. Figure 2 shows the dispersion curve of an SCRLH transmission line and a selection of its resonance modes corresponding to ω_n.

2.1. ZOR Mode Bandwidth Broadening. For $n = 0$, equation (3) yields the following:

$$\omega_{ZOR}^{open} = \omega_0 = \frac{1}{\sqrt{L_L C_R}} = \omega_E, \tag{4}$$

where the superscript open indicates that both ends of the SCRLH transmission line are open circuits. Equation (4) indicates that the ZOR frequency of the SCRLH transmission line is equal to the resonance frequency of the shunt branch of the equivalent circuit. As a result, ω_0 is related only to the values of L_L and C_R and is unrelated to the physical dimension of the SCRLH transmission line. The no-load quality factor Q for an SCRLH transmission line operating in the ZOR mode can also be obtained under the open circuit condition as

$$Q_{ZOR}^{open} = \frac{1/NG}{\omega_{ZOR}^{open}(L_L/N)} = \frac{1}{G}\sqrt{\frac{C_R}{L_L}}, \tag{5}$$

where G is the transmission loss of the shunt branch of the equivalent circuit. Finally, the relationship between the bandwidth BW and the Q factor can be employed to obtain the bandwidth of an SCRLH transmission line operating in the ZOR mode under the open circuit condition as

$$BW^{open} = \frac{1}{Q_{ZOR}^{open}} = G\sqrt{\frac{L_L}{C_R}}. \tag{6}$$

An inspection of equations (4) and (6) indicates that increasing the bandwidth of an SCRLH transmission line operating in the ZOR mode under the open circuit condition

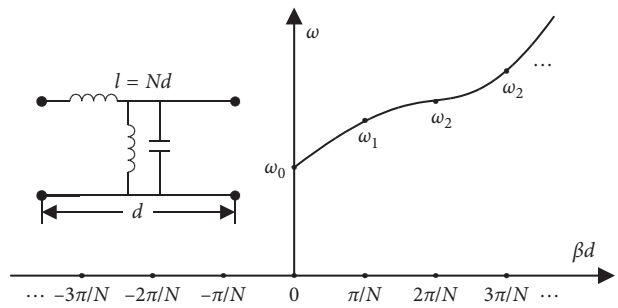

Figure 2: Dispersion curve and corresponding resonance modes of an N-unit SCRLH transmission line of length $l = Nd$.

without changing the resonance frequency requires that L_L be increased and C_R decreased simultaneously while keeping their product constant.

It is also of interest to determine the input impedance of the SCRLH transmission line operating in the ZOR mode under an open circuit condition. Here, one end of the transmission line appears as the input impedance of the other end under the open circuit condition. Therefore, the input impedance of the SCRLH transmission line can be given according to Z and the shunt impedance of the equivalent circuit Y^{-1} as

$$Z_{\text{in}}^{\text{open}} = -jZ_0 \cot^{-1}(\beta l) \overset{\beta \longrightarrow 0}{\approx} -jZ_0 \frac{1}{\beta l} = \frac{1}{NY}. \tag{7}$$

Here, we have substituted $Z_0 = \sqrt{Z/Y}$ and $\gamma = j\beta = \sqrt{ZY}$. This indicates that the input impedance of the entire transmission line is $1/N$ times the shunt impedance of the equivalent circuit.

2.2. FOR Mode Bandwidth Broadening. For $n = 1$ and $N = 3$, equation (3) yields the following:

$$\omega_1 = \sqrt{\frac{1}{C_R}\left(\frac{1}{L_L} + \frac{2}{L_R} - \frac{2}{L_R}\cos\frac{\pi}{N}\right)} = \sqrt{\frac{1}{C_R}\left(\frac{1}{L_L} + \frac{1}{L_R}\right)}. \tag{8}$$

We note here that equations (4) and (8) are of an equivalent form if we substitute the relation

$$\frac{1}{L_s} = \frac{1}{L_L} + \frac{1}{L_R}, \tag{9}$$

into equation (8). In other words, the value of ω_1 for a 3-unit SCRLH transmission line is related only to the values of L_s and C_R and is unrelated to the physical dimension of the SCRLH transmission line. Because FOR occurs when the electrical energy and magnetic energy stored in the resonance cavity are equal, the value of the no-load factor Q under an open circuit condition is given as follows:

$$Q_{\text{FOR}}^{\text{open}} = \omega_{\text{FOR}} \frac{2W_e}{P_{\text{loss}}} = \frac{\omega_{\text{FOR}} C_R}{G} = \frac{1}{G}\sqrt{\frac{C_R(L_R + L_L)}{L_R L_L}}, \tag{10}$$

and the bandwidth of the FOR mode is given by

$$\text{BW}^{\text{open}} = \frac{1}{Q_{\text{FOR}}^{\text{open}}} = G\sqrt{\frac{L_s}{C_R}}. \tag{11}$$

An inspection of equations (9) and (11) indicates that increasing the bandwidth of a 3-unit SCRLH transmission line operating in the FOR mode under the open circuit condition without changing the resonance frequency requires that L_s be increased and C_R decreased simultaneously while keeping their product constant.

The above analysis demonstrates that the resonance frequency of an antenna based on a 3-unit SCRLH transmission line operating in the FOR mode depends only on the parameters of the equivalent circuit, not on its physical dimensions, and therefore differs markedly from conventional half-wavelength microstrip antennas operating in the FOR mode. For this reason, an antenna based on an SCRLH transmission line operating in the FOR mode offers excellent potential for miniaturization.

3. Compact Dual-Frequency Wideband Antenna Based on an SCRLH Transmission Line Operating in ZOR and FOR Modes

3.1. Structural Characteristics and Analysis. To realize the ZOR mode bandwidth broadening principle described above and to match the special case of FOR mode operation with three units, we designed a new CPW structure based on an SCRLH transmission line with Hilbert curve loading. As shown in Figure 3, the CPW is a cascaded structure composed of three SCRLH transmission line units with the same size parameters. The left and right sides are grounded metal plates, and the middle is a radiating metal plate connected to the grounded plate on the right side with metal wires arranged in the shape of a second-order Hilbert curve, which forms the left-handed shunt inductances L_L of the 3-unit SCRLH transmission line. The width of the wires and the distances between the wires are denoted by w_6 and w_7, respectively. In addition, when current is flowing on the middle plate, it inevitably introduces a right-handed inductance L_R. Furthermore, the gap of width w_1 between the grounded plate on the left side and the middle plate results in a distributed right-handed capacitance C_R whose magnitude is inversely proportional to the value of w_1. The other physical dimensions are clearly denoted in the figure.

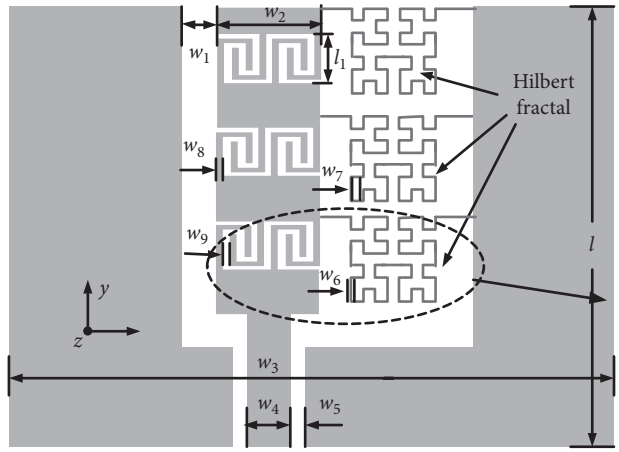

Figure 3: Dual-frequency wideband CPW antenna design based on a 3-unit SCRLH transmission line with Hilbert curve loading.

The Hilbert curve proposed by Hilbert in 1891 is a continuous fractal space-filling curve that fills a two-dimensional plane with one-dimensional line segments. According to its fractal nature, it is characterized by simplicity, self-similarity, and self-avoidance. The formation process is illustrated in Figure 4. The zeroth-order Hilbert curve ($n = 0$) is a line bent into a U-shape, and higher-order curves maintain the same exterior dimensions as the zeroth-order curve. Therefore, the first-order curve ($n = 1$) consists of four U-shaped curves of equivalent exterior dimensions, and their connecting lines are shown as dashed lines in the figure. The second-order curve ($n = 2$) consists of four first-order curves, and their connecting lines are again shown as dashed lines in the figure. This procedure can be repeated indefinitely.

The use of Hilbert curves has been widely reported in microwave antenna applications [10]. Because the magnitude of the inductance of a metal wire is directly proportional to its length and inversely proportional to its width, the use of Hilbert curves effectively extends the wire length over a small area and hence greatly increases the value of L_L. According to the above discussion, suitably increasing the value of L_L can broaden the bandwidth of the antenna under ZOR and FOR mode operation while achieving miniaturization. In addition, we note that the currents in adjacent parallel wires of the Hilbert curve are opposite in direction and may interfere with each other when insufficiently separated. Therefore, taking the effects of manufacturing precision into consideration, we adopted a second-order Hilbert curve with a wire width of $w_6 = 0.3$ mm and an adjacent wire separation of $w_7 = 0.4$ mm. We also note that according to the above discussion, suitably decreasing the value of C_R can broaden the bandwidth of the antenna under ZOR and FOR mode operation while achieving miniaturization, and the value of C_R of the CPW structure is inversely proportional to w_1. Therefore, taking the effects of manufacturing precision into consideration, we adopted a value $w_1 = 3.0$ mm. Compared with a CRLH transmission line structure realized by a conventional microstrip structure, the advantage of using a CPW structure is that it avoids the large plate capacitance between the upper microstrip and the lower metallic grounded plate, although the plate capacitance introduced here cannot be effectively reduced due to the large area of the metallic plate.

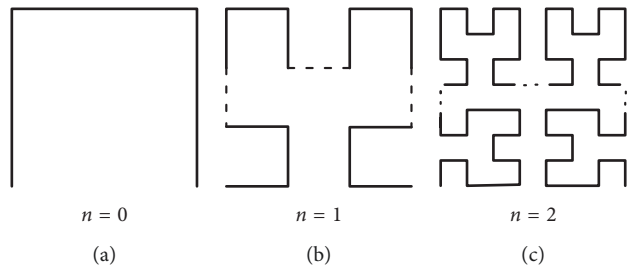

Figure 4: Hilbert curve formation process.

3.2. Simulation and Fabrication of the Antenna Design. A structural model of the proposed antenna design was built and simulated using Ansoft HFSS simulation software to validate the proposed structure and its theoretical analysis and to further investigate its structural characteristics. The parameters were set as $w_1 = 3.0$ mm, $w_2 = 4.6$ mm, $w_3 = 39$ mm, $w_4 = 17.5$ mm, $w_5 = 0.45$ mm, $w_6 = 0.3$ mm, $w_7 = 0.4$ mm, $w_8 = 0.36$ mm, $w_9 = 0.36$ mm, and $l = 24.5$ mm. After initially employing the parameter-scanning function of the simulation software to optimize the design, the value of w_1, related to C_R, was adjusted to 5.7 mm, and w_6 and w_7, related to L_L, were adjusted to 0.3 mm and 0.4 mm, respectively. This process is relatively simple, so it is not described here for the sake of brevity. Finally, in light of engineering requirements, the operating frequency of the antenna was made to cover the WiMax standard (3.5 GHz), and the values of w_2 and l were adjusted to achieve impedance matching.

A prototype antenna was fabricated based on the optimized antenna design parameters to further validate the proposed design. The dielectric board used for the CPW was

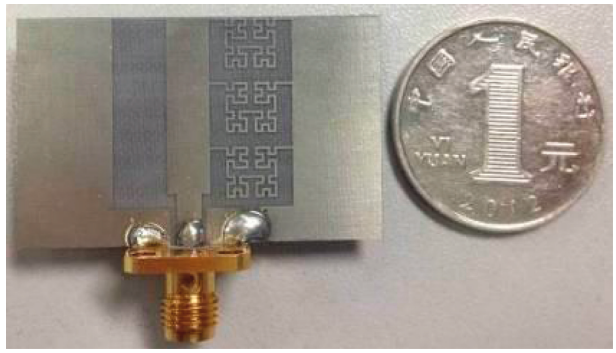

Figure 5: Prototype ZOR mode and FOR mode dual-frequency wideband antenna based on a 3-unit SCRLH transmission line with Hilbert curve loading.

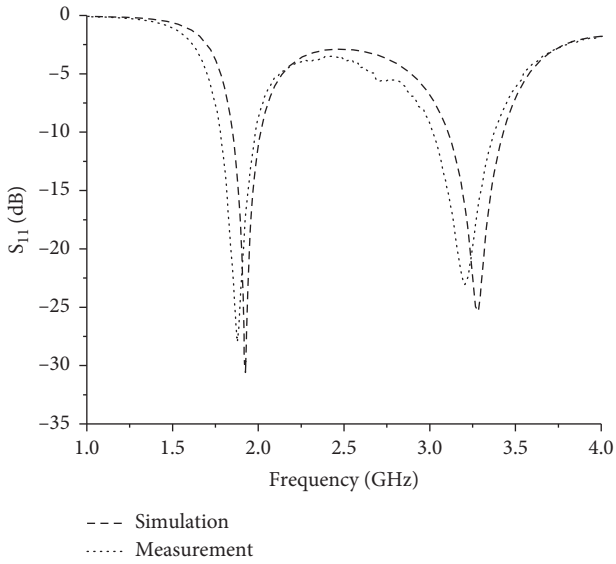

Figure 6: Simulation and experimental results of the return loss for the proposed ZOR and FOR dual-frequency wideband antenna.

a polytetrafluoroethylene glass scrim board (F4B-2) with a relative dielectric constant of 2.65 and a thickness of 1 mm. Figure 5 presents an image of the prototype antenna. The overall dimensions of the antenna for the ZOR mode are $0.24\lambda_0 \times 0.15\lambda_0 \times 0.006\lambda_0$. The electrical dimensions of the SCRLH transmission line unit structure are even smaller, indicating a high degree of miniaturization.

Figure 6 presents the simulation and experimental results of the return loss for the proposed ZOR and FOR mode dual-frequency wideband antenna. The figure shows that the proposed antenna provided center frequencies of $f_0 = 1.865$ GHz and $f_1 = 2.835$ GHz, and that the -10 dB return loss bandwidths for the ZOR and FOR modes were, respectively, 187 MHz (from 1.773 GHz to 1.96 GHz) and 368 MHz (from 3.002 GHz to 3.37 GHz). The corresponding relative bandwidths were, respectively, 10.1% and 11.5%. In addition, we note that the experimental results were in excellent agreement with the simulation results. The designed antenna can therefore be applied to multiple wireless communication systems simultaneously.

Figure 7 presents the simulation and experimental results of the directivity patterns of the antenna gain for f_0 (ZOR mode) and f_1 (FOR mode) center frequencies under copolarization (Co-pol) and cross-polarization (X-pol) conditions in the *yoz* and *xoy* planes. As shown in Figures 7(a) and 7(c), the radiation directivity pattern of the antenna in the *yoz* plane is relatively uniform under Co-pol conditions, and omnidirectional radiation is realized over the entire operating frequency band. Furthermore, as shown in Figures 7(b) and 7(d), the directivity patterns under Co-pol conditions in the *xoy* plane present standard figure, eight shapes with a horizontal deviation less than 15° over the entire operating frequency band, which are similar to the radiation directivity pattern of a dipole antenna. We also note that the cross-polarization of the antenna is also small. The experimental and simulated peak gains in the *yoz* and *xoy* planes are essentially equivalent at both f_0 and f_1. The experimental peak gains at f_0 and f_1 are 1.54 dB and 1.71 dB, respectively, which are very close to the

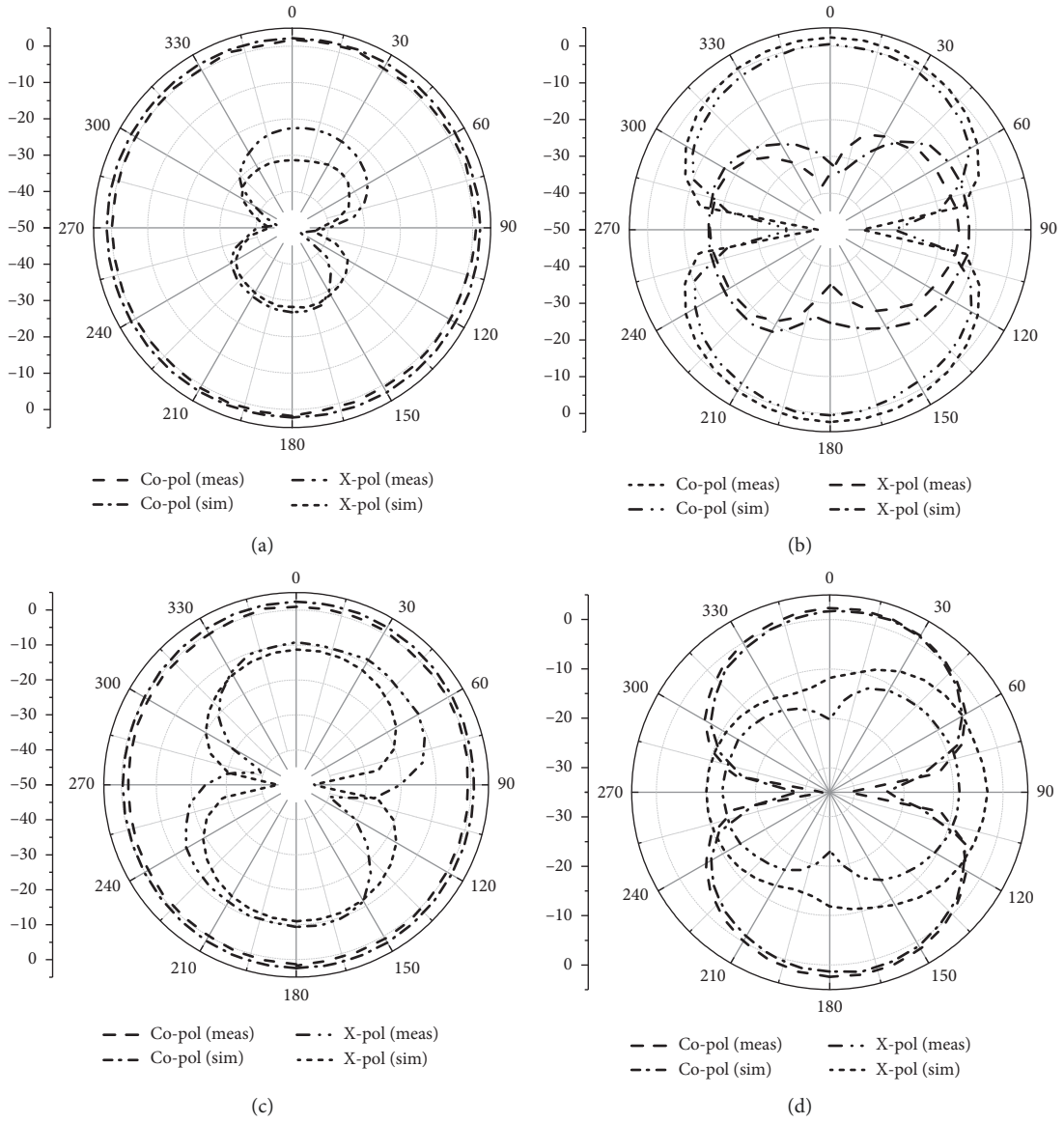

Figure 7: Simulated and measured directivity patterns of the ZOR mode (center frequency $f_0 = 1.865$ GHz) and FOR mode (center frequency $f_1 = 2.835$ GHz) dual-frequency wideband antenna. In the *yoz* plane (H-plane): (a) f_0; (c) f_1. In the *xoy* plane (E-plane): (b) f_0; (d) f_1.

corresponding simulated peak gains of 1.86 dB and 1.97 dB. The radiation efficiency of the antenna is also very good, and the efficiencies for the ZOR and FOR modes are 79.3% and 74.2%, respectively. In contrast, with a conventional half-wave resonant microstrip patch antenna, where the phase lag can cause excessive current concentration and high conductor loss, the conductor loss of the proposed antenna operating in the ZOR mode due to the metal patch is small because the antenna has a uniform amplitude and in-phase electric field distribution. The antenna therefore increases the radiation efficiency in the ZOR mode and alleviates to some extent the gain and radiation efficiency reduction due to miniaturization.

The performance parameters of the wideband dual-frequency antenna designed in this paper are summarized in Table 1, which includes the operating frequency, bandwidth, peak gain, and radiation efficiency. F.O.M. is the ESA figure-of-merit (=G_ant/(VSWR × L)). $L = D$/lambda and D is the maximum dimension of the antenna, and lambda is the wavelength for the lowest frequency, and VSWR is the 10 dB bandwidth. To further illustrate the performance advantages of the proposed antenna, Table 1 includes the reported performance parameters of previously proposed antenna designs based on the CRLH transmission line structure. The results indicate that the antenna designed in this paper offers considerable advantages in terms of expanded bandwidth and higher gain and efficiency.

Table 1: Comparison of the performance parameters of the antenna designed in this paper with those of other antenna designs presented in the literature.

Comparison category	This work		Narbudowicz et al. [4]		Jang et al. [11]	Lai et al. [12]
Electronic size	$0.24\lambda_0 \times 0.15\lambda_0 \times 0.006\lambda_0$		$0.28\lambda_0 \times 0.28\lambda_0 \times 0.006\lambda_0$		$0.145\lambda_0 \times 0.172\lambda_0 \times 0.011\lambda_0$	$0.33\lambda_0 \times 0.33\lambda_0 \times 0.018\lambda_0$
Transmission line	APW SCRLH		CRLH		CRLH	CRLH
With/without through holes	Without		With		Without	With
Mode of operation	ZOR	FOR	ZOR	FOR	ZOR	ZOR
Operating frequency (GHz)	1.867	2.835	1.329	2.756	2.03	3.38
Relative bandwidth (%)	10.1	11.5	1.35	2.02	6.8	0.1
Peak gain (dB)	1.86	1.97	−0.7	−0.2	1.35	0.87
F.O.M.	0.0409	0.0129	−0.16	−0.007	0.058	1.524
Radiation efficiency (%)	81.3	74.2	Not given		62	70

4. Conclusions

This paper proposed a new wideband dual-frequency CPW antenna design based on an SCRLH transmission line structure with Hilbert curve loading. The multifrequency characteristics of the SCRLH transmission line structure were evaluated theoretically, and the antenna parameters promoting bandwidth broadening under ZOR and FOR mode operation were evaluated. The analysis revealed that the bandwidth broadening of the ZOR and FOR modes is independent of the antenna length, and the SCRLH transmission line structure therefore facilitates wideband operation under miniaturization. Finally, the proposed dual-frequency ZOR and FOR mode antenna design was validated by the excellent agreement between the simulation results and experimental results for a highly compact prototype antenna. The bandwidth, gain, and efficiency of the antenna were demonstrated to be superior to those obtained by antennas based on the CRLH transmission line structure.

Data Availability

The data used to support the findings of this study are available from the corresponding author upon request.

Conflicts of Interest

The authors declare no conflicts of interest.

Acknowledgments

This research was supported by PLA Strategic Support Army Information Engineering University.

References

[1] C. Caloz and T. Itoh, *Electromagnetic Metamaterials: Transmission Line Theory and Microwave Applications*, John Wiley & Sons, Hoboken, NJ, USA, 2006.

[2] B.-C. Park and J.-H. Lee, "Dual-band omnidirectional circularly polarized antenna utilizing epsilon negative transmission line," in *Proceedings of the 2012 Asia Pacific Microwave Conference*, pp. 82–84, Kaohsiung, Taiwan, December 2012.

[3] H.-X. Xu, G.-M. Wang, and M.-Q. Qi, "A miniaturized triple-band metamaterial antenna with radiation pattern selectivity and polarization diversity," *Progress In Electromagnetics Research*, vol. 137, pp. 275–292, 2013.

[4] A. Narbudowicz, X. L. Bao, and M. J. Ammann, "Dual-band omnidirectional circularly polarized antenna," *IEEE Transactions on Antennas and Propagation*, vol. 61, no. 1, pp. 77–83, 2013.

[5] S. Narieda, S. Tanaka, Y. Ido et al., "Planar dual band omnidirectional UHF antennas employing a composite right/left handed double-sided metal layer structure," in *Proceedings of the IEEE Radion and Wireless Symposium*, p. 143, San Diego, CA, USA, January 2009.

[6] A. Gummalla, M. Achour, G. Poilasne et al., "Compact dual band planar metamaterial antenna arrays for wireless LAN," in *Proceedings of the IEEE Antennas and Propagation Society International Symposium*, p. 1, San Diego, CA, USA, July 2008.

[7] X. Q. Xian Qi Lin, R. P. Ruo Peng Liu, X. M. Xin Mi Yang et al., "Arbitrarily dual-Band components using simplified structures of conventional CRLH TLs," *IEEE Transactions on Microwave Theory and Techniques*, vol. 54, no. 7, pp. 2902–2909, 2006.

[8] W. Han and Y. Feng, "Ultra-wideband bandpass filter using simplified left-handed transmission line structure," *Microwave and Optical Technology Letters*, vol. 50, no. 11, pp. 2758–2762, 2008.

[9] J.-H. Park, Y.-H. Ryu, J.-G. Lee, and J.-H. Lee, "Epsilon negative zeroth-order resonator antenna," *IEEE Transactions on Antennas and Propagation*, vol. 55, no. 12, pp. 3710–3712, 2007.

[10] T. P. Li, G. M. Wang, J. G. Liang et al., "Novel composite right/left handed transmission-line and its application on filter design," *Acta Physica Sinica*, vol. 61, no. 19, Article ID 194201, 2012.

[11] T. Jang, J. Choi, and S. Lim, "Compact coplanar waveguide (CPW)-Fed zeroth-order resonant antennas with extended Bandwidth and high efficiency on vialess single layer," *IEEE Transactions on Antennas and Propagation*, vol. 59, no. 2, pp. 363–372, 2011.

[12] A. Lai, K. M. K. H. Leong, and T. Itoh, "Infinite wavelength resonant antennas with monopolar radiation pattern based on periodic structures," *IEEE Transactions on Antennas and Propagation*, vol. 55, no. 3, pp. 868–876, 2007.